Mass Distributions in Clusters of Galaxies:

X–Ray and Lensing Comparisons of 2 Intermediate–Redshift CNOC Clusters

Amalia K. Hicks & Erica Ellingson (CASA, University of Colorado Boulder)

ABSTRACT

Assuming hydrostatic equilibrium, X–ray observations can be used to derive estimates for the masses of clusters of galaxies. Such estimates provide an independant check on masses derived from optical gravitational lensing. It is common to find discrepancies between lensing and X–ray derived masses, in part because ofthe low spatial resolution of previous X–ray missions. The motivation of this study is a search for evidence of excess mass in the cores of clusters, in addition to that predicted by a single beta–model. We discuss results from an analysis of two Chandra observations of clusters in the CNOC sample. We present estimates for the cluster masses and compare these results to estimates from gravitational lens data taken from the literature.

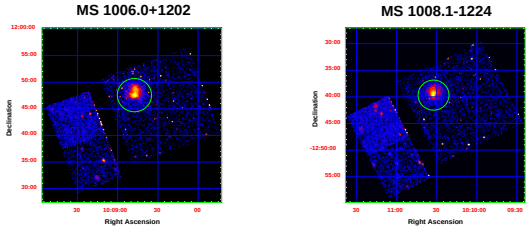

Figure 1 : Extended Images. Extended flux images of the ACIS-I observations of MS 1006.0+1202 and MS 1008.1-1224 for the 0.3-7.0 keV band. A circle of 1 Mpc radius is centered on the X-ray peak of each cluster. These images correspond to 25.6 ksec and 37.4 ksec exposure times, respectively.

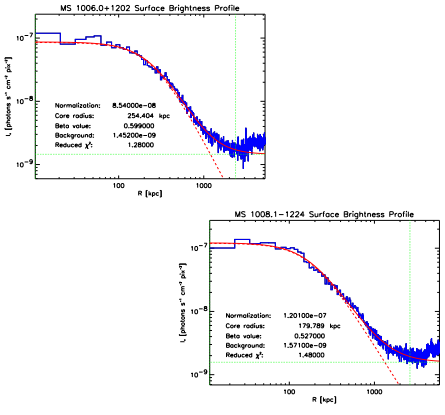

Figure 2 : Surface Brightness Profiles. Radial surface brightness profiles for the 0.3-7.0 keV band accumulated in 2 arcsec annular bins. The data is shown in blue and the corresponding β model fit in red. The resulting values for the core radius and β parameter are indicated. The vertical green dashed indicates the outer limits of the data included in the fit while the horizontal green lines indicates the determined background level.

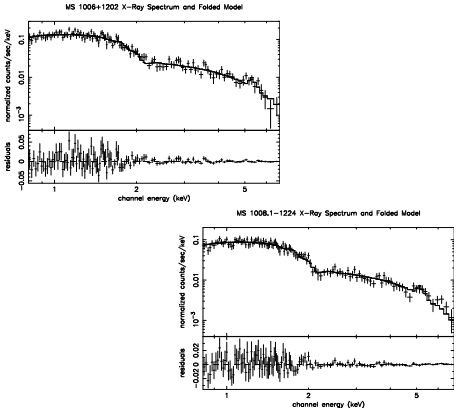

Figure 3 : Spectral Fits. Representative cluster spectra accumulated within elliptical apertures centered on the peak of the X-ray emission and with a major axis of 500 kpc. These spectra were fit with a single temperature MEKAL model, which yielded temperatures of 8.5 and 8.6 keV, abundances of 0.25 and 0.31, and reduced chi-squareds of 1.024 and 0.8372 respectively for MS 1006.0+1202 and MS 1008.1-1221.

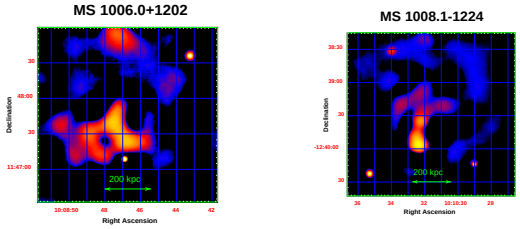

Figure 4 : Core Substructure. Adaptively smoothed flux images of MS 1006.0+1202 and MS 1008.1-1224. Smooth surface brightness models have been subtracted to enhance the X-ray substructure in the cores.

Summary

- Spectral fitting indicates that the clusters are best described by a single temperature model. Abundances of 0.25 and 0.31 (similar to those found in low redshift clusters) were obtained for MS 1006.0+1202 and MS 1008.1-1224, respectively.
- We derive total gravitating masses of $13.58 \times 10^{14} M_{\odot}$ and $13.52 \times 10^{14} M_{\odot}$ within R_{200}, numbers nearly consistent with dynamical mass estimates.
- Imaging reveals significant substructure throughout the cluster.
- Using a beta model fit and mean cluster temperature, we derive cluster masses we derive mass estimates which are a factor of 2-3 smaller than gravitational lensing estimates (Molikawa et al. 1996), implying that:
- The equilibrium dark matter distribution may follow a steeper profile than a beta-model (Eke, Navarro & Frenk, 1998).
- Mass determination through gas may be complicated by substructure (Allen 1998).
- Improvements of up to a factor of two may come from the determination of arc redshifts, and more detailed analysis of core substructure.

Table 1. Mass Estimates

Cluster	Redshift	$R_{2\,\mathrm{Mpc}}$ [h_{73}^{-1} Mpc]	kT_X [keV]	$M^X_{\mathrm{gas},2\,\mathrm{Mpc}}$ [$10^{13} M_{\odot}$]	$M^X_{\mathrm{tot},2\,\mathrm{Mpc}}$ [$10^{13} M_{\odot}$]	$M^{\mathrm{dyn}}_{2\,\mathrm{Mpc}}$ [$10^{13} M_{\odot}$]
MS 1006.0+1202	0.2605	2.44	$8.5^{+.1}_{-.1}$	$23.18^{+4.24}_{-4.24}$	$135.83^{+23.27}_{-23.27}$	138^{+28}_{-28}
MS 1008.1-1224	0.3062	2.72	$8.66^{+.1}_{-.1}$	$30.24^{+4.23}_{-4.23}$	$135.17^{+21.27}_{-21.27}$	$200^{+\infty}_{-88}$

Mass Comparisons

Cluster	R_{arc} [arcsec]	f_{gas}	$\frac{M_{\mathrm{gas}}}{M_{\mathrm{tot}}}$	$M_X(<R_{arc})$ [$10^{13} M_{\odot}$]	$M_{\mathrm{Lens}}(<R_{arc})$ [$10^{13} M_{\odot}$]	$\frac{M_{\mathrm{Lens}}}{M_X}$
MS 1006.0+1202	26	0.170654	1.01598	$5.30^{+2.3}_{-2.6}$	12.0	2.22635
MS 1008.1-1224	47	0.223718	1.47962	$17.01^{+.35}_{-.37}$	55.0	3.23339

References

Allen, S.W. 1998, MNRAS, 296, 392
Allen, S.W., Schmidt, R.W. & Fabian, A.C. 2002, astro-ph 0111368
Carlberg, R.G. et al. 1996, ApJ, 462, 32
Eke, V.R., Navarro, J.F. & Frenk, C.S. 1998, ApJ, 503, 569
Lewis, A.D. et al. 1999, ApJ, 517, 587
Molikawa, K. et al. 1999, A&A, 351, 413
Stocke, J.T. et al. 1999, AJ, 117, 1967
Wu, X. 2000, MNRAS, 316, 299